DOI: 10.1021/om100103u

ORGANOMETALLICS
Article

Bioinspired Catalytic Conjugate Additions of Thiophenols to α,β-Enones by a Disubstituted Benzoate-Bridged Nickel Mimic for the Active Site of Urease

Way-Zen Lee,*[,†] Huan-Sheng Tseng,[†] Tzu-Li Wang,[†] Hui-Lien Tsai,*[,‡] and Ting-Shen Kuo[§]

[†]*Department of Chemistry, National Taiwan Normal University, Taipei 11650, Taiwan,* [‡]*Department of Chemistry, National Cheng Kung University, Tainan 70101, Taiwan, and* [§]*Instrumentation Center, Department of Chemistry, National Taiwan Normal University, Taipei 11650, Taiwan*

Received February 10, 2010

A disubstituted benzoate polydentate ligand, 2,6-bis[bis(pyridinyl-2-methyl)aminoethoxyl]benzoate (H**L**), was prepared to synthesize nickel mimics for the active site of urease. Reaction of the deprotonated $\mathbf{L}^-$ with $Ni(ClO_4)_2\cdot 6H_2O$ afforded a dinickel complex, $[\mathbf{L}Ni_2(CH_3CN)(THF)](ClO_4)_3$ (**1**), characterized by UV/vis spectroscopy and X-ray crystallography. Addition of urea to an acetonitrile solution of **1** afforded a dinickel urea adduct, $[\mathbf{L}Ni_2(urea)_2](ClO_4)_3\cdot 2CH_3CN$ (**2**), which was structurally and spectroscopically characterized. ^{1}H NMR and ESI-MS spectra of **2** both evidenced that urea molecules remained coordinated to the nickel centers of **2** in solution. With the inspiration of urea coordination to the nickel centers of **1**, the conjugate additions of thiophenols to α,β-enones catalyzed by complex **1** were examined and found to proceed in good yields. In contrast, the same catalytic reaction by $Ni(ClO_4)_2\cdot 6H_2O$ and H**L** was far less effective. Also, addition of NaOAc or $NaOAcPh_2$ to an acetonitrile solution of **1** gave tetranuclear nickel complexes, $[\mathbf{L}Ni_2(\mu\text{-}OAc)]_2(ClO_4)_4\cdot 3H_2O$ (**3**) and $[\mathbf{L}Ni_2(\mu\text{-}OAcPh_2)]_2(ClO_4)_4\cdot 5CH_3CN\cdot 2THF$ (**4**), and their molecular structures determined by X-ray diffraction can be described as dimers of dimers. Each dinickel core of **3** and **4** closely mimics the active site of urease. The magnetic data of **1**, **3**, and **4** exhibited a very weak antiferromagnetic coupling ($J = -0.72$ cm^{-1} for **1**, -0.65 cm^{-1} for **3** and **4**) between two metal centers in the dinickel core.

Urease, which can catalyze the hydrolysis of urea, exists in a variety of bacteria, fungi, and higher plants[1] and permits the organism to consume external or internal generated urea as a nitrogen source.[2] Hydrolysis of urea catalyzed by the dinickel active site of urease produces CO_2 and 2 equiv of NH_3.[1] The degradation rate of urea by the enzyme is 10^{14} times faster than its spontaneous decomposition rate.[3] Due to this fast catalysis, soil bacterial urease can rapidly hydrolyze fertilizer urea to unproductive volatilized ammonia and cause the damage of plants.[2] Also, the existence of urease in *Helicobacter pylori*, which causes gastric inflammation and peptic ulcer disease, allows the bacteria to survive in the gastric mucosa of patients at acidic pH.[4] Two enzymatic mechanisms of urease have been proposed,[5,6] and the first intermediate in both mechanisms is the urea-bound enzyme, in which urea is proposed to coordinate to the nickel center in the active site of urease. Many reported protein structures of urease with high resolution[7] reveal that two nickel ions exist in the active site of the enzyme with a separation of 3.5 Å. The

*To whom correspondence should be addressed. E-mail: wzlee@ntnu.edu.tw.

(1) Hausinger, R. P. *Biochemistry of Nickel*; Plenum Press: New York, 1993; Chapter 3.

(2) (a) Mobley, H. L.T.; Hausinger, R. P. *Microbiol. Rev.* **1989**, *53*, 85–108. (b) Zonia, L. E.; Stebbins, N. E.; Polacco, J. C. *Plant Physiol.* **1995**, *107*, 1097–1103.

(3) Blakeley, R. L.; Treston, A.; Andrews, R. K.; Zerner, B. *J. Am. Chem. Soc.* **1982**, *104*, 612–614.

(4) Mobley, H. L. T.; Island, M. D.; Hausinger, R. P. *Microbiol. Rev.* **1995**, *59*, 415–480.

(5) (a) Karplus, P. A.; Pearson, M. A.; Hausinger, R. P. *Acc. Chem. Res.* **1997**, *30*, 330–337. (b) Benini, S.; Ciurli, S.; Rypniewski, W. R.; Wilson, K. S.; Mangani, S. *Acta Crystallogr., Sect. D: Biol. Crystallogr.* **1998**, *54*, 409–412. (c) Benini, S.; Rypniewski, W. R.; Wilson, K. S.; Miletti, S.; Ciurli, S.; Mangani, S. *Struct. Fold. Des.* **1999**, *7*, 205–216. (d) Benini, S.; Rypniewski, W. R.; Wilson, K. S.; Ciurli, S.; Mangani, S. *J. Biol. Inorg. Chem.* **2001**, *6*, 778–790. (e) Musiani, F.; Arnolfi, E.; Casadio, R.; Ciurli, S. *J. Biol. Inorg. Chem.* **2001**, *6*, 300–314. (f) Pearson, M. A.; Michel, L. O.; Hausinger, R. P.; Karplus, P. A. *Biochemistry* **1997**, *36*, 8164–8172. (g) Pearson, M. A.; Schaller, R. A.; Michel, L. O.; Karplus, P. A.; Hausinger, R. P. *Biochemistry* **1998**, *37*, 6214–6220. (h) Todd, M. J.; Hausinger, R. P. *Biochemistry* **2000**, *39*, 5389–5396. (i) Pearson, M. A.; Prk, I.-S.; Schaller, R. A.; Michel, L. O.; Karplus, P. A.; Hausinger, R. P. *Biochemistry* **2000**, *39*, 8575–8584.

(6) (a) Fearon, W. R. *Biochem. J.* **1923**, *17*, 84–93. (b) Mack, E.; Villars, D. S. *J. Am. Chem. Soc.* **1923**, *45*, 505–510. (c) Meyer, F.; Kaifer, E.; Kircher, P.; Heinze, K.; Pritzkow, H. *Chem. Eur. J.* **1999**, *5*, 1617–1630. (d) Barrios, A. M.; Lippard, S. J. *J. Am. Chem. Soc.* **2000**, *122*, 9172–9177. (e) Estiu, G.; Merz, K. M., Jr. *J. Am. Chem. Soc.* **2004**, *126*, 11832–11842.

(7) (a) Jabri, E.; Carr, M. B.; Hausinger, R. P.; Karplus, P. A. *Science* **1995**, *268*, 998–1004. (b) Park, I.-S.; Michel, L. O.; Pearson, M. A.; Jabri, E.; Karplus, P. A.; Wang, S.; Dong, J.; Scott, R. A.; Koehler, B. P. *J. Biol. Chem.* **1996**, *271*, 18632–18637. (c) Pearson, M. A.; Michel, L. O.; Hausinger, R. P.; Karplus, P. A. *Biochemistry* **1997**, *36*, 8164–8172. (d) Benini, S.; Rypniewski, W. R.; Wilson, K. S.; Miletti, S.; Ciurli, S.; Mangani, S. *Structure* **1999**, *7*, 205–216. (e) Ha, N. C.; Oh, S. T.; Sung, J. Y.; Cha, K. A.; Lee, M. H.; Oh, B. H. *Nat. Struct. Biol.* **2001**, *8*, 505–509.

 Published on Web 06/08/2010

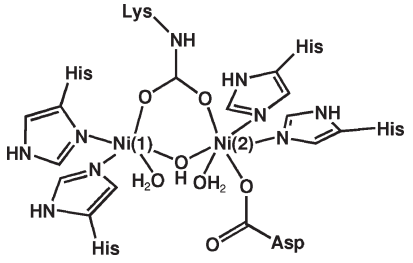

Figure 1. Schematic representation of the active site of urease.

two nickel ions are bridged by a rather unusual carbamate group, which is converted from the reaction of Lys[217] with carbon dioxide, and a hydroxide group.[7a] It has been confirmed that the binding of nickel ions into the active site of the apoenzyme of urease requires the presence of carbon dioxide.[8] Each nickel is coordinated by two histidine residues and a water molecule, resulting in a distorted-square-pyramidal geometry for Ni(1), and Ni(2) is terminally ligated to an additional aspartate residue, forming a pseudooctahedral ligand environment (Figure 1). Many model complexes for the active site of urease have been reported,[9−12] but only a few nickel mimics were bridged by a disubstituted benzoate polydentate ligand. Recently, we reported two dinickel mimics, $[L^1Ni_2(DMF)_4](ClO_4)_3$ and $[L^2Ni_2(CH_3CN)_4](ClO_4)_3$ (where L^1 = 2,6-bis[bis(pyridinyl-2-methyl)aminomethyl]benzoate and L^2 = 2,6-bis[bis(1-methylbenzimidazolyl-2-methyl)aminomethyl]benzoate), in which urea can coordinate to the nickel centers of the complexes.[13] Due to the short length of the ligand side arms of L^1 and L^2, the conformation of the dinickel core of the two mimics becomes W-shaped, and the Ni···Ni distances of such complexes are much longer than that in the active site of urease. In order to obtain nickel complexes which possess a dinickel core with a Ni···Ni distance similar to that of the active site of urease, synthesis of a new ligand is indispensable. A disubstituted benzoate with longer side arms, 2,6-bis[(2-bis-(2-pyridylmethyl)aminoethoxy)]benzoic acid (H**L**; Chart 1), was synthesized by modifying a reported method.[14] Herein, we demonstrate the synthesis of a dinickel complex, $[LNi_2(CH_3CN)(THF)](ClO_4)_3$ (**1**), bridged by the disubstituted benzoate **L** and its ability to bind urea forming a urea adduct, $[LNi_2(urea)_2](ClO_4)_3\cdot 2CH_3CN$ (**2**). As a result of urea coordination to the nickel centers of **2**, we were inspired to examine the catalysis of conjugate addition of thiophenols to α,β-enones by the dinickel complex **1** and found much higher yields compared to those by $Ni(ClO_4)_2\cdot 6H_2O$ and H**L**. In addition, complex **1** can react with NaOAc and $NaOAcPh_2$ to form two nickel mimics, $[LNi_2(\mu\text{-}OAc)]_2(ClO_4)_4$ (**3**) and $[LNi_2(\mu\text{-}OAcPh_2)]_2(ClO_4)_4$ (**4**), which possess dinickel cores having coordination environments similar to that of the active site of urease. The magnetic properties of complexes **1**, **3**, and **4** were studied.

Chart 1

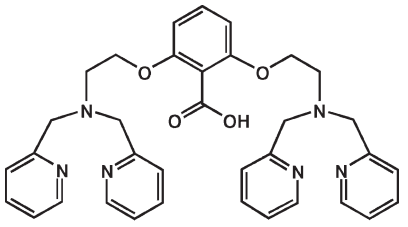

H**L**

Results and Discussion

Synthesis and Spectroscopic Characterization of the Dinickel Urea Adduct. In order to construct nickel mimics possessing a coordination environment similar to that of the active site of urease, a disubstituted benzoate ligand, H**L**, which comprises side arms longer than those of the previous ligands, L^1 and L^2,[13] was prepared by modification of a reported method.[14] The prepared H**L** was deprotonated by sodium methoxide in methanol to form a pale yellow solution, which was subsequently transferred into an acetonitrile solution of $Ni(ClO_4)_2\cdot 6H_2O$ to form a light blue solution. The light blue product was purified and recrystallized by the slow diffusion method (THF/CH_3CN). Nice needlelike crystals of $[LNi_2(CH_3CN)(THF)](ClO_4)_3$ (**1**) were obtained in 73% yield. Reaction of complex **1** with excess urea in acetonitrile afforded a dinickel urea adduct, $[LNi_2(urea)_2](ClO_4)_3\cdot 2CH_3CN$ (**2**), in which each nickel center of the complex was coordinated by a urea molecule. Complex **2** was fully characterized by IR, ^1H NMR, and ESI-MS spectroscopy. The solid FTIR spectrum (KBr pellet) of **2** exhibited the stretching frequency for the carbonyl group of the bound urea at 1662 cm^{-1} shifted from that of free urea at 1690 cm^{-1}. The ^1H NMR spectra of complexes **1** and **2** showed relatively sharp resonance signals for high-spin six-coordinated dinickel(II) species (Figure 2).[13,15] In comparison to the spectrum of **1**, a pronounced signal for the bound urea molecules in the spectrum of **2** was observed at 4.69 ppm, an upfield shift from 4.81 ppm (free urea in CD_3CN). In addition, the ESI-MS spectrum of **2** indicated that urea molecules remained coordinated on the nickel centers of **2** in solution (ESI-MS (m/z, amu): 440 for $[LNi_2(urea)(ClO_4)]^{2+}$). Since the geometry of the nickel centers in **2** remained the same as that in **1**, the electronic absorption spectra of **1** and **2** exhibited similar absorption bands of three weak d−d transitions in the visible region. In spite of saturated coordination on the nickel centers of **1**, the nickel ions of **1** could bind urea to form the urea adduct of **2**. The coordination of urea to the nickel centers of **2** is due to the electronic deficiency of the dinickel core. With the inspiration of urea coordination to the nickel centers of **2**, the catalytic conjugate additions of thiophenols to α,β-enones by complex **1** were investigated.

(8) Park, I.-S.; Hausinger, R. P. *Science* **1995**, *267*, 1156–1158.
(9) (a) Barrios, A. M.; Lippard, S. J. *J. Am. Chem. Soc.* **1999**, *121*, 11751–11757. (b) Barrios, A. M.; Lippard, S. J. *J. Am. Chem. Soc.* **2000**, *122*, 9172–9177.
(10) (a) Meyer, F.; Kaifer, E.; Kircher, P.; Heinze, K.; Pritzkow, H. *Chem. Eur. J.* **1999**, *5*, 1617–1630. (b) Meyer, F.; Pritzkow, H. *Chem. Commun.* **1998**, 1555–1556.
(11) (a) Buchanan, R. M.; Mashuta, M. S.; Oberhausen, K. J.; Richardson, J. F.; Li, Q.; Hendrickson, D. N. *J. Am. Chem. Soc.* **1989**, *111*, 4497–4498. (b) Koga, T.; Furutachi, H.; Nakamura, T.; Fukita, N.; Ohba, M.; Takahashi, K.; Okawa, H. *Inorg. Chem.* **1998**, *37*, 989–996. (c) Carlsson, H.; Haukka, M.; Bousseksou, A.; Latour, J.; Nordlander, E. *Inorg. Chem.* **2004**, *43*, 8252–8262. (d) Uozumi, S.; Furutachi, H.; Ohba, M.; Okawa, H.; Fenton, D. E.; Shindo, K.; Murata, S.; Kitko, D. J. *Inorg. Chem.* **1998**, *37*, 6281–6287.
(12) (a) Yamaguchi, K.; Koshino, S.; Akagi, F.; Suzuki, M.; Uehara, A.; Suzuki, S. *J. Am. Chem. Soc.* **1997**, *119*, 5752–5753. (b) Volkmer, D.; Hommerich, B.; Griesar, K.; Haase, W.; Krebs, B. *Inorg. Chem.* **1996**, *35*, 3792–3803.
(13) Lee, W.-Z.; Tseng, H.-S.; Ku, M.-Y.; Kuo, T.-S. *Dalton Trans.* **2008**, 2538–2541.
(14) Gutkina, E. A.; Trukhan, V. M.; Pierpont, C. G.; Mkoyan, S.; Strelets, W.; Norlander, E. *Dalton Trans.* **2006**, 492–501.
(15) Belle, C.; Bougault, C.; Averbuch, M.-T.; Durif, A.; Pierre, J.-L.; Latour, J.-M.; Le Pape, L. *J. Am. Chem. Soc.* **2001**, *123*, 8053–8066.

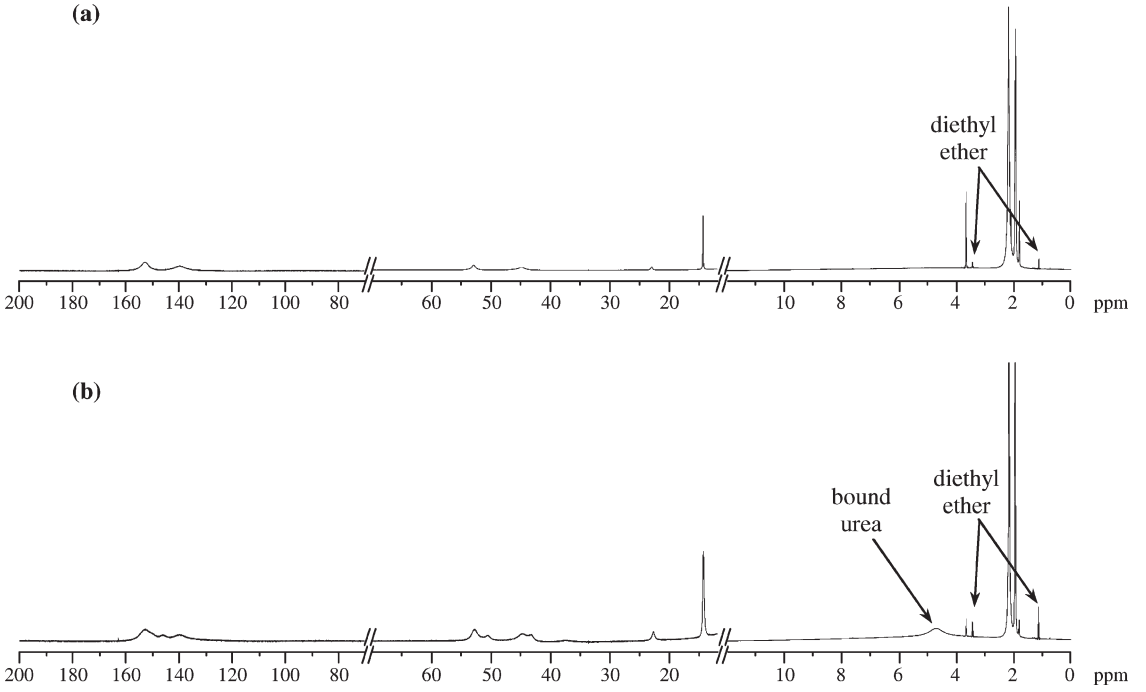

Figure 2. ^{1}H NMR spectra of (a) $[LNi_2(CH_3CN)(THF)](ClO_4)_3$ (**1**) and (b) $[LNi_2(urea)_2](ClO_4)_3$ (**2**).

Catalytic Studies. Conjugate addition of thiols to α,β-unsaturated carbonyl compounds (thia-Michael addition) is one of the most important synthetic strategies for C−S bond formation.[16] Several metal complexes have been reported to facilitate the thia-Michael addition.[17] Only a few nickel complexes have shown the capability of catalyzing such conjugate additions.[18] Recently, we have reported a low-coordinated nickel bis(benzimidazoyl) complex, which possessed effective catalysis toward the conjugate additions of thiophenols to α,β-enones.[18a] To extend this study, we further examined the catalytic ability of complex **1** for the previous reactions. 2-Cyclohexenone (**5**) was first selected as a test Michael acceptor, and 4-methoxythiophenol (**10**) was employed as a test Michael donor in the presence of catalyst **1**. An almost quantitative yield of 3-(4-methoxyphenylsulfanyl)-cyclohexenone was produced in 2 h by using 1 mol% of **1** in acetonitrile (0.25 M) at room temperature (Table 1, entry 1). Under the same reaction conditions, $Ni(ClO_4)_2\cdot 6H_2O$ and

Table 1. Thia-Michael Addition of Thiophenols to α,β-Enones

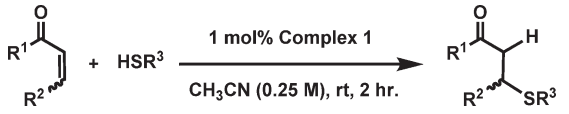

Entry	Michael acceptor	Michael donor	Yield (%)
1[a]	 **5**	4-$CH_3OC_6H_4SH$	96 (**5a**)
2	**5**	4-$CH_3C_6H_4SH$	43 (**5b**)
3	**5**	C_6H_5SH	41 (**5c**)
4	**5**	4-$NO_2C_6H_4SH$	34 (**5d**)
5	 **6**	4-$CH_3OC_6H_4SH$	41 (**6a**)
6	**6**	4-$CH_3C_6H_4SH$	21 (**6b**)
7	**6**	C_6H_5SH	12 (**6c**)
8	**6**	4-$NO_2C_6H_4SH$	41 (**6d**)
9	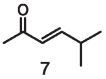 **7**	4-$CH_3OC_6H_4SH$	33 (**7a**)
10	**7**	4-$CH_3C_6H_4SH$	8 (**7b**)
11	**7**	C_6H_5SH	5 (**7c**)
12	**7**	4-$NO_2C_6H_4SH$	trace (**7d**)

[a] Yield of the reaction catalyzed by $Ni(ClO_4)_2\cdot 6H_2O$: 64%; by H**L**: 33%.

H**L** were examined as control catalysts to evaluate the catalytic ability of complex **1**. The yields of the same reaction catalyzed by $Ni(ClO_4)_2\cdot 6H_2O$ and by H**L** are 64% and 33%, respectively. Apparently, complex **1** behaves as a more effective catalyst for the conjugate additions of thiophenols to α,β-enones. With this preliminary success, thia-Michael additions to other Michael acceptors such as 3-pentenone (**6**) and 5-methyl-3-hexenone (**7**) by 4-methoxythiophenol and

(16) (a) Fluharty, A. L. In *The Chemistry of the Thiol Group*; Patai, S., Ed.; Wiley: New York, 1974; Part 2, p 589. (b) Clark, J. H. *Chem. Rev.* **1980**, *80*, 429–452. (c) Fujita, E.; Nagao, Y. J. *Bioorg. Chem.* **1977**, *6*, 287–309. (d) Trost, B. M.; Keeley, D. E. *J. Org. Chem.* **1975**, *40*, 2013–2013. (e) Shono, T.; Matsumura, Y.; Kashimura, S.; Hatanaka, K. *J. Am. Chem. Soc.* **1979**, *101*, 4752–4753. (f) Nishimura, K.; Ono, M.; Nagaoka, Y.; Tomioka, K. *J. Am. Chem. Soc.* **1997**, *119*, 12974–12975.

(17) (a) Kondo, T.; Mitsudo, T.-A. *Chem. Rev.* **2000**, *100*, 3205–3220. (b) Saito, M.; Nakajima, M.; Hashimoto, S. *Chem. Commun.* **2000**, 1851–1852. (c) Emori, E.; Arai, T.; Sasai, H.; Shibasaki, M. *J. Am. Chem. Soc.* **1998**, *120*, 4043–4044. (d) Delp, S. A.; Munro-Leighton, C.; Goj, L. A.; Ramirez, M. A.; Gunnoe, T. B.; Petersen, J. L.; Boyle, P. D. *Inorg. Chem.* **2007**, *46*, 2365–2367. (e) Bandini, M.; Cozzi, P. G.; Giacomini, M.; Melchiorre, P.; Selva, S.; Umani-Ronchi, A. *J. Org. Chem.* **2002**, *67*, 3700–3704. (f) Srivastava, N.; Banik, B. K. *J. Org. Chem.* **2003**, *68*, 2109–2114. (g) Ranu, B. C.; Mandal, T. *Synlett* **2004**, 1239–1242. (h) Kawatsura, M.; Komatsu, Y.; Yamamoto, M.; Hayase, S.; Itoh, T. *Tetrahedron* **2008**, *64*, 3488–3493. (i) Matsumoto, K.; Watanabe, A.; Uchida, T.; Ogi, K.; Katsuki, T. *Tetrahedron Lett.* **2006**, *47*, 1291–1293. (j) Garg, S. K.; Kumar, R.; Chakraborti, A. K. *Tetrahedron Lett.* **2005**, *46*, 1721–1724.

(18) (a) Lee, W.-Z.; Wang, T.-L.; Tseng, H.-S.; Liu, C.-Y.; Chen, C.-T.; Kuo, T.-S. *Organometallics* **2009**, *28*, 652–655. (b) Evans, D. A.; Seidel, D. *J. Am. Chem. Soc.* **2005**, *127*, 9958–9959. (c) Kanemasa, S.; Oderaotoshi, Y.; Wada, E. *J. Am. Chem. Soc.* **1999**, *121*, 8675–8676.

Table 2. Thia-Michael Addition of Thiophenols to Cycloenones

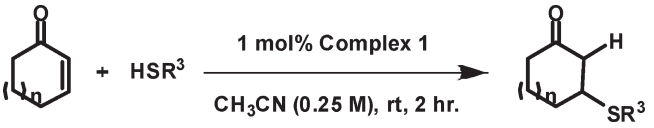

entry	Michael acceptor	Michael donor	yield (%)
		$n = 1$	
1	**5**	4-$CH_3OC_6H_4SH$	96 (**5a**)
2	**5**	3-$CH_3OC_6H_4SH$	78 (**5d**)
3	**5**	2-$CH_3OC_6H_4SH$	58 (**5e**)
		$n = 0$	
4	**8**	4-$CH_3OC_6H_4SH$	74 (**8a**)
5	**8**	3-$CH_3OC_6H_4SH$	77 (**8d**)
6	**8**	2-$CH_3OC_6H_4SH$	51 (**8e**)
		$n = 2$	
7	**9**	4-$CH_3OC_6H_4SH$	89 (**9a**)
8	**9**	3-$CH_3OC_6H_4SH$	86 (**9d**)
9	**9**	2-$CH_3OC_6H_4SH$	81 (**9e**)

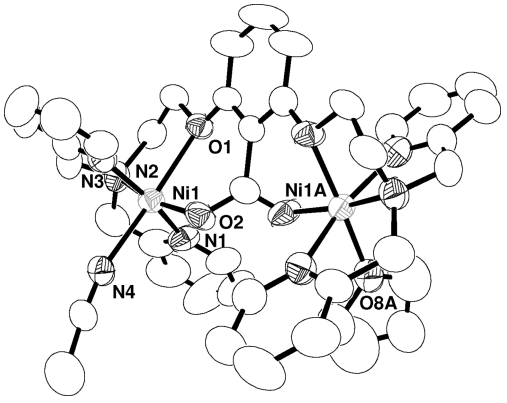

Figure 3. Thermal ellipsoid representation of [$\mathbf{L}Ni_2(CH_3CN)$-(THF)]$(ClO_4)_3$ (**1**) at the 50% probability level. Hydrogen atoms, solvent molecules, and the counteranions of **1** are omitted for clarity. Selected bond lengths for **1**: Ni1−N1 = 2.062 Å, Ni1−N2 = 2.053 Å, Ni1−N3 = 2.027 Å, Ni1−N4 = 2.104 Å, Ni1−O1 = 2.173 Å, Ni1−O2 = 1.970 Å, Ni1A-O8A = 2.095 Å.

its three derivatives, 4-(methylthio)phenol, thiophenol, and 4-(nitrothio)phenol, were further explored. When the nucleophilicity of thiophenols is decreased by installing an electron-withdrawing substituent at the para position of thiophenols, the yields for the conjugate additions are decreased (Table 1, entries 1−4). In addition, if the β-position of the alkene moiety in the enones is more sterically hindered, the yields of the conjugate additions are also decreased (Table 1, entries 1, 5, and 9). As represented in the thia-Michael additions to substrate **7**, the reaction rates drop by 3−10 times. The data given in Table 1 clearly reveal that the yield for the thia-Michael addition of 4-methoxythiophenol to cyclohexenone (Table1, entry 1) is much superior to those for other thia-Michael addition combinations. Therefore, the conjugate additions of 4-, 3-, or 2-(methoxythio)phenols to cycloenones with different ring sizes were further investigated. When the methoxy substituent of the Michael donor (methoxythio)phenol was changed from the para to the ortho position, the yields of the conjugate additions dropped dramatically from 96% to 58% (Table 2, entries 1−3).

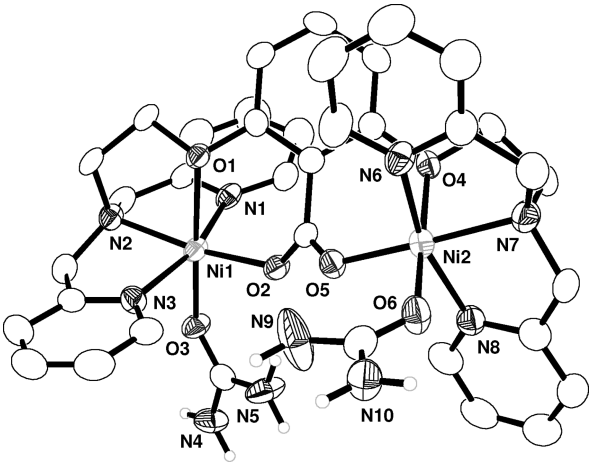

Figure 4. Thermal ellipsoid representation of [$\mathbf{L}Ni_2(urea)_2$]$(ClO_4)_3$ (**2**), at the 50% probability level. Hydrogen atoms, solvent molecules, and the counteranions of **2** are omitted for clarity. Selected bond lengths for **2**: Ni1−N1 = 2.059 Å, Ni1−N2 = 2.043 Å, Ni1−N3 = 2.081 Å, Ni1−O1 = 2.197 Å, Ni1−O2 = 1.985 Å, Ni1−O3 = 2.031 Å, Ni2−N6 = 2.057 Å, Ni2−N7 = 2.047 Å, Ni2−N8 = 2.076 Å, Ni2−O4 = 2.184 Å, Ni2−O5 = 1.978 Å, Ni2−O6 = 2.034 Å.

Obviously, the decrease in reaction yield is caused by the steric hindrance of the methoxy group of (methoxythio)phenol on meta and ortho positions. In the case of the system for 4-, 3-, and 2-(methoxythio)phenols and 2-cyclopentenone (**8**), the individual yields of the conjugate additions were lower than those for the system of 2-cyclohexenone, specifically for 4-(methoxythio)-phenol (Table 2, entries 4−6). Also, the reaction yields did not follow their trend of bulkiness. The yield for entry 5 is higher than that for entry 4. This result may be rationalized by the stronger nucleophilicity of 3-(methoxythio)phenol compared to that of 4-(methoxythio)phenol. For the system of 2-cycloheptenone, the yields of the Michael products for entries 7−9 in Table 2 are similar. This phenomenon could be attributed to the flexibility of the large ring size of cycloheptene. The overall result suggests that complex **1** serves as an effective catalyst for the conjugate additions of thiophenols to α,β-enones.

X-ray Structures of Nickel Complexes. The X-ray structure of complex **1** reveals a dinickel complex, in which two nickel ions are bridged by the central benzoate group of **L** (Figure 3). Each nickel ion is coordinated by three nitrogen donors, i.e. one amine and two pyridines, from a side arm of **L** and a solvent molecule, CH_3CN or THF. In addition, the oxygen atoms of the ether groups in **L** coordinate to the nickel centers, causing complex **1** to form a W-shaped dinickel core with a Ni···Ni separation of 5.8 Å. Both nickel ions possess a distorted-octahedral geometry, and the three nitrogen donors occupy the meridional plane of the nickel coordination sphere. Complex **2** was also structurally characterized by X-ray crystallography. The molecular structure of **2** is similar to that of **1** (Figure 4). The dinickel core of **2** is W-shaped with a Ni···Ni separation of 5.88 Å.

Addition of acetate or diphenylacetate to an acetonitrile solution of **1** afforded the tetranuclear nickel complexes [$\mathbf{L}Ni_2(\mu\text{-}OAc)]_2(ClO_4)_4$ (**3**) and [$\mathbf{L}Ni_2(\mu\text{-}OAcPh_2)]_2(ClO_4)_4$ (**4**), respectively. The molecular structures of **3** and **4** (Figure 5), determined by X-ray crystallography, display an arrangement of a dimer of dimers.[11c,13] Each dimer consists of two nickel ions which are symmetrically bridged by an acetate in **3** or a diphenylacetate in **4** and asymmetrically

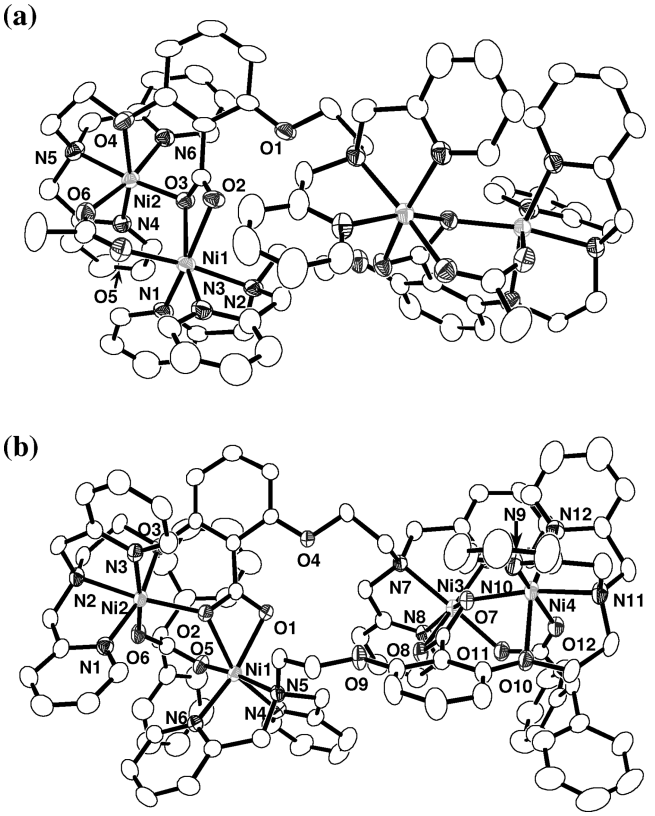

Figure 5. Thermal ellipsoid representations of (a) $[LNi_2(\mu\text{-OAc})]_2(ClO_4)_4$ (**3**), and (b) $[LNi_2(\mu\text{-OAcPh}_2)]_2(ClO_4)_4$ (**4**) at the 50% probability level. Hydrogen atoms, solvent molecules, and the counteranions of **3** and **4** are omitted for clarity. Selected bond lengths for **3**: Ni1−N1 = 2.055 Å, Ni1−N2 = 2.138 Å, Ni1−N3 = 2.044 Å, Ni1−O2 = 2.162 Å, Ni1−O3 = 2.173 Å, Ni1−O5 = 2.000 Å, Ni2−N4 = 2.039 Å, Ni2−N5 = 2.062 Å, Ni2−N6 = 2.062 Å, Ni2−O3 = 2.010 Å, Ni2−O4 = 2.176 Å, Ni2−O6 = 2.048 Å. Selected bond lengths for **4**: Ni1−N4 = 2.036 Å, Ni1−N5 = 2.142 Å, Ni1−N6 = 2.037 Å, Ni1−O1 = 2.145 Å, Ni1−O2 = 2.187 Å, Ni1−O5 = 1.998 Å, Ni2−N1 = 2.040 Å, Ni2−N2 = 2.064 Å, Ni2−N3 = 2.041 Å, Ni2−O2 = 2.003 Å, Ni2−O3 = 2.154 Å, Ni2−O6 = 2.059 Å, Ni3−N7 = 2.137 Å, Ni3−N8 = 2.031 Å, Ni3−N9 = 2.051 Å, Ni3−O7 = 2.172 Å, Ni3−O8 = 2.151 Å, Ni3−O11 = 1.998 Å, Ni4−N10 = 2.052 Å, Ni4−N11 = 2.062 Å, Ni4−N12 = 2.044 Å, Ni4−O7 = 2.008 Å, Ni4−O10 = 2.192 Å, Ni4−O12 = 2.049 Å.

bridged by the central benzoate group of **L**. As acetate or diphenylacetate replaced the bound solvent molecule on the nickel center of **1**, one ether oxygen atom of the side arm of **L** and the central benzoate were dissociated from the nickel center of the dinuclear **1**, forming an open dimer. Subsequently, a dimer of dimers was constructed by the coordination of the acetate or diphenylacetate to the benzoate bound nickel center of an adjacent open dimer and the bidentate bonding of the central benzoate from the adjacent open dimer to the nickel center of the first open dimer (Scheme 1). In addition to the similarity of the first coordination sphere of the dinickel core of **3** or **4** to that of the active site of urease, we notice that the distance between two nickel ions in the dinickel cores of **3** and **4** is about 3.7 Å, similar to that in the enzyme (Figure 6).

Magnetic Properties. The magnetic properties of polycrystalline samples of **1**, **3**, and **4** have been studied at 1 kG over temperatures ranging from 1.8 to 300.0 K. The product $\chi_M T$ per nickel dimer, where χ_M is the molar magnetic susceptibility,

Scheme 1

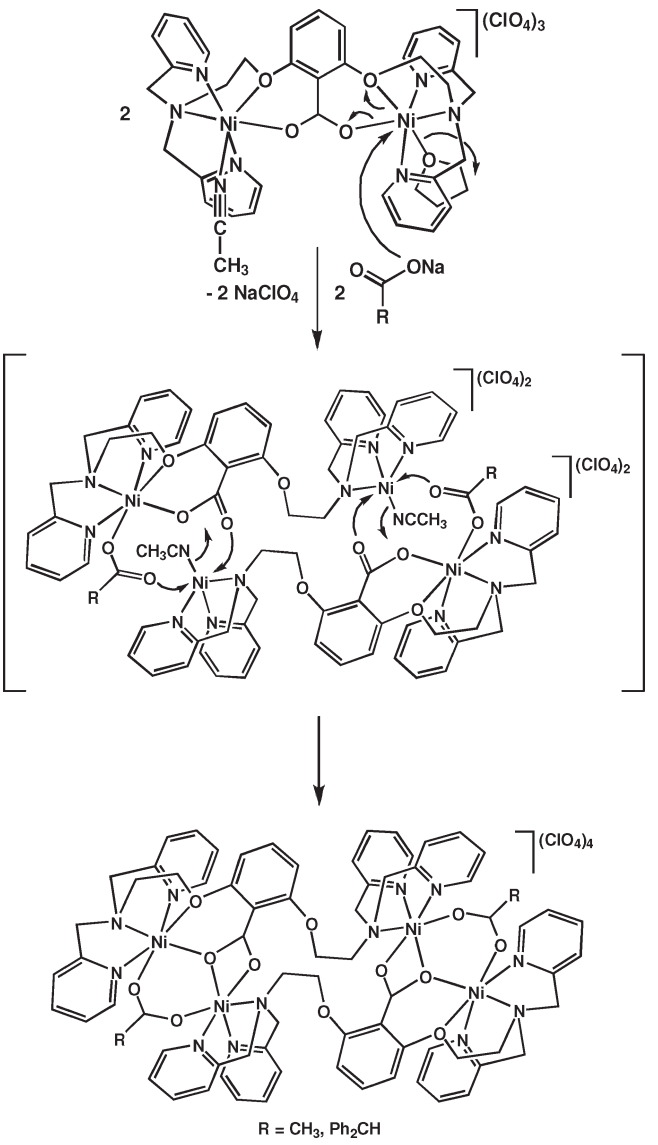

and $1/\chi_M$ per nickel versus temperature for complexes **1**, **3**, and **4** are given in Figures 7 and 8, respectively. The values of $\chi_M T$ for complexes **1**, **3**, and **4** were 2.60, 2.38, and 2.26 $cm^3\ mol^{-1}$ K at 300.0 K, respectively, and gradually decreased upon cooling to 2.40, 2.06, and 2.16 $cm^3\ mol^{-1}$ K at 30.0 K. After the temperature was lowered to 30.0 K, the values rapidly decreased to 0.96, 0.92, and 1.02 $cm^3\ mol^{-1}$ K at 1.8 K. The observed $\chi_M T$ change over temperature is a typical behavior of the antiferromagnetically coupled magnetic pair. The magnetic exchange coupling between the nickel centers for complexes **1**, **3**, and **4** was analyzed on the basis of the Curie−Weiss expression and a dimer magnetic model. The effective magnetic moment (μ_{eff}) was obtained from the slope of those plots in the high-temperature region, in which the data obey the Curie−Weiss law, $\chi_M = C/(T - \Theta) = N\mu_{eff}^2/3k(T - \Theta)$, where C, Θ, N, and k are the Curie, Weiss, Avogadro, and Boltzmann constants, respectively. All three data sets follow a linear Curie−Weiss law behavior, and the effective magnetic moments (μ_{eff}) per Ni ion and Weiss constants for complexes **1**, **3**, and **4** can be determined. The effective magnetic moments per Ni of complexes **1**, **3**, and **4** are 3.24, 3.06, and 3.01 μ_B, respectively, which are typical

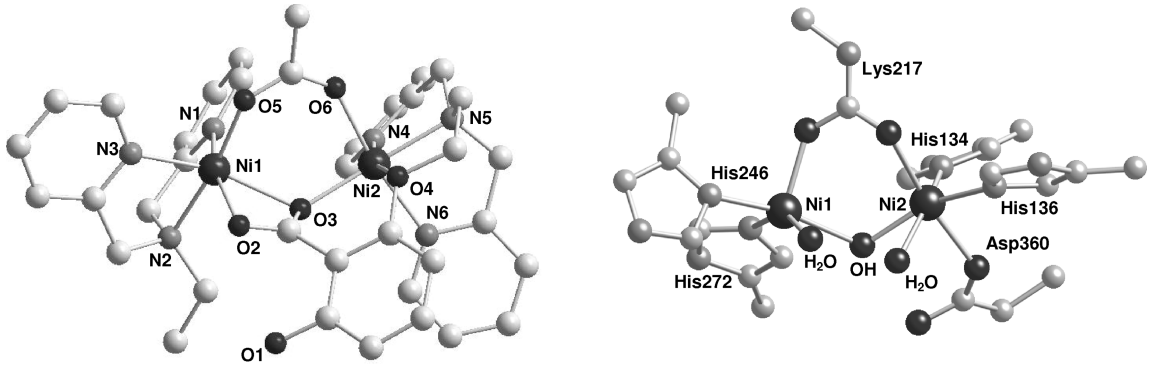

Figure 6. Ball and stick representations of a dimer moiety in **3** (left) and the active site of urease (right).

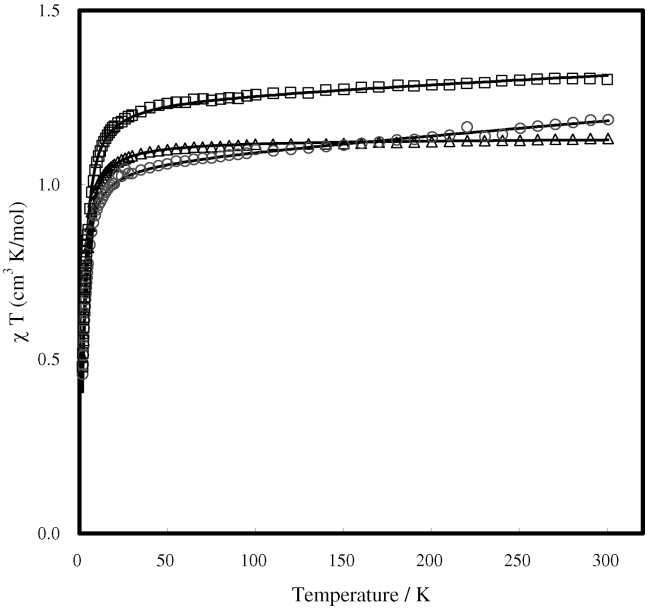

Figure 7. Plots of the product of molar magnetic susceptibilities with temperature, $\chi_M T$, versus temperature for polycrystalline samples of complexes **1** (□), **3** (○), and **4** (△). The solid lines are the best fits for eq 1.

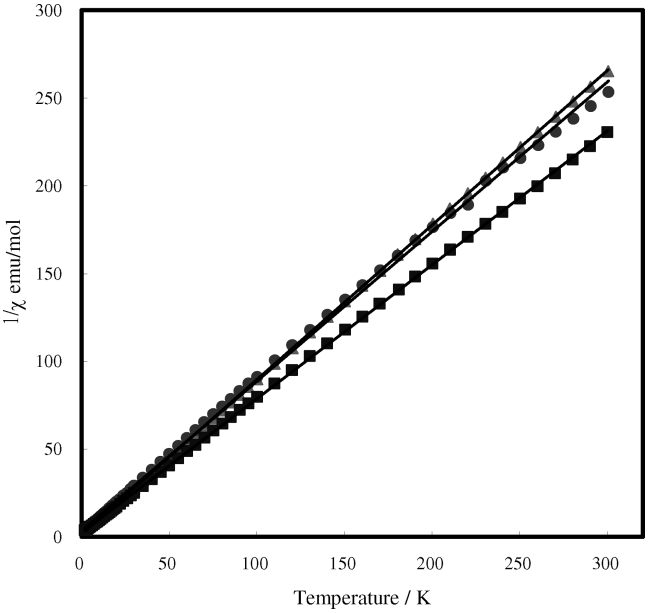

Figure 8. Plots of inverse magnetic susceptibilities ($1/\chi_M$) versus temperature for polycrystalline samples of complexes **1** (■), **3** (●), and **4** (▲). The solid lines are best linear fits for the Curie−Weiss law.

values of six-coordinated Ni(II) and establish $^3A_2$ ground states. The values of μ_{eff} are larger than the spin-only value of 2.83 μ_B, and these are commonly observed for the Ni(II) centers due to incomplete quenching and arise from the spin−orbital coupling. The Weiss constants are −2.95, −3.95, and −1.75 K for complexes **1**, **3**, and **4**, respectively. The negative Θ values indicate antiferromagnetic exchange interactions between nickel centers.

The magnetic interactions between the nickel centers can be treated as a nickel dimer model. Assuming an isotropic model, the exchange expression for two equivalent $S = 1$ ions based on the spin Hamiltonian, $H = -2JS_1 \cdot S_2$, is given by

$$\chi_M = \frac{Ng^2\beta^2}{kT}\frac{2\exp(2J/kT) + 10\exp(6J/kT)}{1 + 3\exp(2J/kT) + 5\exp(6J/kT)} + \text{TIP} \quad (1)$$

The symbols N, β, g and k have their usual meanings. J represents the exchange coupling interaction, and TIP is the temperature-independent paramagnetism of nickel dimer centers. Least-squares fitting of eq 1 to the experimental data $\chi_M T$ per nickel dimer versus temperature for complexes **1**, **3**, and **4** are illustrated in Figure 7. The magnetic parameters obtained are as follows: for complex **1**, $g = 2.24$, $J = -0.72$ cm^{-1} and TIP $= 4.9 \times 10^{-4}$ emu mol^{-1}; for complex **3**, $g = 2.06$, $J = -0.65$ cm^{-1}, and TIP $= 8.4 \times 10^{-4}$ emu mol^{-1}; for complex **4**, $g = 2.13$, $J = -0.65$ cm^{-1}, and TIP $= 2.4 \times 10^{-5}$ emu mol^{-1}. Such a weak antiferromagnetic interaction was also observed in the active site of urease.[19] Although the Ni···Ni separation is shorter for complexes **3** and **4** than for complex **1**, the carboxylate bridge ligands are not good pathways for magnetic coupling, and antiferromagnetic interaction constants of the three complexes are near −0.7 cm^{-1}.

Concluding Remarks

The dinickel complex **1** coordinated by solvent molecules, CH_3CN and THF, was synthesized by reacting the disubstituted benzoate $\mathbf{L}^-$ with $Ni(ClO_4)_2 \cdot 6H_2O$. The labile coordination of CH_3CN and THF in **1** allows the coordination of urea or anionic OAc^- or $OAcPh_2^-$ to the nickel centers of **1**

(19) Clark, P. A.; Wilcox, D. E. *Inorg. Chem.* **1989**, *28*, 1326–1333.

Table 3. Selected X-ray Crystallographic Data for Complexes 1−4

	1	2	3	4
empirical formula	$C_{41}H_{46}Cl_2N_7Ni_2O_{13}$	$C_{41}H_{49}Cl_3N_{12}Ni_2O_{18}$	$C_{74}H_{84}Cl_4N_{12}Ni_4O_{31}$	$C_{116}H_{123}Cl_4N_{17}Ni_4O_{30}$
fw	1033.17	1221.69	2014.17	2611.95
T (K)	200(2)	200(2)	200(2)	200(2)
cryst syst	monoclinic	monoclinic	monoclinic	monoclinic
space group	$C2/c$	$C2/c$	$C2/c$	$P2_1/c$
a (Å)	30.6691(5)	26.8326(12)	21.0070(3)	23.8448(2)
b (Å)	9.5065(2)	26.1759(12)	34.1810(6)	20.2926(2)
c (Å)	18.3372(4)	17.3070(8)	16.9250(4)	24.8296(2)
α (deg)	90	90	90	90
β (deg)	114.5660(10)	119.0910(10)	112.1910(10)	96.57
γ (deg)	90	90	90	90
V (Å^3)	4862.38(17)	10622.4(8)	11252.7(4)	11935.50(18)
Z	4	8	4	4
D_{calcd} (g/cm^3)	1.411	1.528	1.189	1.454
μ (mm^{-1})	0.951	0.941	0.822	0.795
cryst size (mm)	0.48 × 0.30 × 0.15	0.24 × 0.15 × 0.06	0.45 × 0.40 × 0.40	0.25 × 0.20 × 0.10
goodness of fit F^2	1.111	1.103	1.059	1.018
R1	0.0664	0.0619	0.0722	0.0645
wR2	0.2044	0.1666	0.2194	0.1614

to form the urea adduct of **2** or tetranuclear **3** or **4**. For the urea adduct of **2**, both ^{1}H NMR and ESI-MS spectra have evidenced that the bound urea molecules did not dissociate from the nickel centers of the complex in solution. The coordination of urea in **2** suggests that nucleophiles, such as α,β-enones or thiols, could also bind to the nickel centers of **1**. The conjugate additions of thiophenols to α,β-enones catalyzed by complex **1** was observed, and the yield of the thia-Michael additions is mainly governed by the steric hindrance of α,β-enones and the nucleophilicity of thiophenols. Notably, the dinickel cores of **3** and **4** structurally mimic the active site of urease.

Experimental Section

Methods and Materials. All manipulations were performed under nitrogen using standard Schlenk techniques. Methanol was dried over magnesium iodide prior to use. Acetonitrile was distilled once from P_2O_5 and freshly distilled from CaH_2 before use. Dichloromethane was distilled from CaH_2 before use. Diethyl ether and THF were dried by distillation from sodium benzophenone prior to use. All reagents were obtained from commercial sources and used as received without further purification. UV−vis spectra were recorded on Hitachi U-3501 spectrophotometers. IR spectra were recorded using KBr pellets on a Perkin-Elmer Paragon 500 spectrometer. NMR spectra were recorded on Bruker Avance-400 MHz FT NMR spectrometers. ESI-MS spectra were recorded on a Thermo Finnigan LCQ Advantage spectrometer. Elemental analyses for C, H, and N were performed on a Perkin-Elmer 2400 analyzer at the NSC Regional Instrumental Center at National Taiwan University, Taipei, Taiwan.

2,6-Bis[(2-bis(2-pyridylmethyl)aminoethoxy)]benzoic Acid (HL). H**L** was prepared by adopting a reported method.[14] ^{1}H NMR (400 MHz, $CDCl_3$, ppm): 8.33−8.32 (m, 4H, Ar), 7.69−7.64 (m, 8H, Ar), 7.08−7.07 (m, 4H, Ar), 6.93 (t, 1H, Ar, J = 8.4 Hz), 6.21 (d, 2H, Ar, J = 8.4 Hz), 4.06 (t, 4H, CH_2, J = 4.4 Hz), 3.98 (s, 8H, CH_2), 3.03 (t, 4H, CH_2, J = 4.4 Hz). ^{13}C NMR (100 MHz, $CDCl_3$, ppm): 167.9, 159.4, 155.7, 148.3, 137.3, 130.3, 123.8, 122.3, 116.3, 104.7, 66.6, 60.7, 53.4. ESI-MS (m/z, amu): 605 $[M + H]^+$.

$[LNi_2(CH_3CN)(THF)](ClO_4)_3$ (1). NaOMe (0.0577 g, 1.07 mmol) was added to a methanol solution (80 mL) of H**L** (0.6471 g, 1.07 mmol) and reacted for 2 h. The reaction mixture was then added to an acetonitrile solution (15 mL) of $Ni(ClO_4)_2\cdot 6H_2O$ (0.7818 g, 1.07 mmol) to form a light blue solution. After the mixture was stirred for 2 h, the solvent of the blue solution was removed under vacuum to give a blue residue. The residue was washed by THF (80 mL × 3) to remove $NaClO_4$. The blue product of **1** was isolated and dissolved in acetonitrile for recrystallization by the slow diffusion of THF into the acetonitrile solution at ambient temperature. Blue crystals were obtained in 1 week in 73% yield (0.8864 g). Anal. Calcd for $[LNi_2(CH_3CN)(THF)](ClO_4)_3$ ($Ni_2C_{41}H_{46}N_7Cl_3O_{17}$): C, 43.48; H, 4.09; N, 8.66. Found: C, 43.12; H, 4.06; N, 8.92. UV−vis (CH_3CN, λ_{max}, nm (ε, cm^{-1} M^{-1})): 361 (88), 564 (40), 860 (42). IR (KBr, cm^{-1}): 2061 (ν_{CN}), 1605 (ν_{py}), 1560 (ν_{py}), 1446, 1397, 1291, 1146 ($\nu_{ClO_4^-}$), 1117 ($\nu_{ClO_4^-}$), 1086 ($\nu_{ClO_4^-}$), 766, 727, 635 ($\nu_{ClO_4^-}$), 627 ($\nu_{ClO_4^-}$). ESI-MS (m/z, amu): 919 $[LNi_2(ClO_4)_2]^+$, 410 $[LNi_2(ClO_4)]^{2+}$, 254 $[LNi_2(CH_3CN)]^{3+}$, 240 $[LNi_2]^{3+}$.

$[LNi_2(urea)_2](ClO_4)_3\cdot 2CH_3CN$ (2). Urea (0.0242 g, 0.4 mmol) was dissolved in methanol (10 mL) and transferred into a blue acetonitrile solution (10 mL) of complex **1** (0.2264 g, 0.2 mmol). The reaction mixture was stirred for 2 h; then the solvent of the resulting mixture was removed under vacuum to give a blue residue. The resulting residue was dissolved in acetonitrile for recrystallization by the slow diffusion of diethyl ether into the acetonitrile solution of **2** at ambient temperature. Light blue crystals were obtained in 1 week in 67% yield (0.1558 g). Anal. Calcd for $[LNi_2(urea)_2](ClO_4)_3\cdot CH_3CN$ ($Ni_2C_{39}H_{46}N_{11}Cl_3O_{18}$): C, 39.68; H, 3.93; N, 13.05. Found: C, 39.29; H, 4.12; N, 13.14. mp: 212−214 °C. UV−vis (CH_3CN, λ_{max}, nm (ε, cm^{-1} M^{-1})): 362sh (78), 573 (42), 894 (42). IR (KBr, cm^{-1}): 3204 (ν_{NH}), 1662 (ν_{CO}), 1651 (ν_{COO^-}), 1632 (ν_{COO^-}), 1606 (ν_{py}), 1557 (ν_{py}), 1446, 1399, 1240, 1144 ($\nu_{ClO_4^-}$), 1116 ($\nu_{ClO_4^-}$), 1088 ($\nu_{ClO_4^-}$), 766, 636 ($\nu_{ClO_4^-}$), 627 ($\nu_{ClO_4^-}$). ESI-MS (m/z, amu): 919 $[LNi_2(ClO_4)_2]^+$, 440 $[LNi_2(urea)(ClO_4)]^{2+}$, 410 $[LNi_2(ClO_4)]^{2+}$, 240 $[LNi_2]^{3+}$.

$[LNi_2(\mu\text{-}OAc)]_2(ClO_4)_4\cdot 3H_2O$ (3). NaOAc (0.0164 g, 0.2 mmol) was dissolved in 10 mL of methanol and transferred into an acetonitrile solution (30 mL) of complex **1** (0.2264 g, 0.2 mmol) to form a light blue solution. The reaction mixture was stirred for 2 h. The solvent of the resulting mixture was then removed under vacuum to give a blue residue. The residue was washed by THF (40 mL × 3) to remove $NaClO_4$. The blue product of **3** was isolated and dissolved in acetonitrile for recrystallization by the slow diffusion of THF into the acetonitrile solution at ambient temperature. Light blue crystals were obtained for 1 week in 78% yield (0.1588 g). Anal. Calcd for $[LNi_2(\mu\text{-}OAc)]_2(ClO_4)_4\cdot 3H_2O$ ($Ni_4C_{74}H_{84}N_{12}Cl_4O_{31}$): C, 44.13; H, 4.21; N, 8.35. Found: C, 44.46; H, 4.70; N, 8.62. Mp: 282−284 °C. UV−vis (CH_3CN, λ_{max}, nm (ε, cm^{-1} M^{-1})): 358 sh (70), 587 (64), 1003 (58). IR (KBr, cm^{-1}): 3401 (ν_{OH}), 1607 (ν_{py}), 1574 (ν_{py}), 1483, 1446, 1382, 1242, 1146 ($\nu_{ClO_4^-}$), 1114 ($\nu_{ClO_4^-}$), 1089 ($\nu_{ClO_4^-}$), 1026, 767, 636 ($\nu_{ClO_4^-}$), 626 ($\nu_{ClO_4^-}$). ESI-MS (m/z, amu): 879 $[L_2Ni_4(\mu\text{-}OAc)_2(ClO_4)_2]^{2+}$, 553 $[L_2Ni_4(\mu\text{-}OAc)_2(ClO_4)]^{3+}$, 390 $[L_2Ni_4(\mu\text{-}OAc)_2]^{4+}$.

$[LNi_2(\mu\text{-}OAcPh_2)]_2(ClO_4)_4\cdot 5CH_3CN\cdot 2THF$ (4). The preparation of complex **4** was the same as for complex **3**. Light blue crystals of **4** were obtained in 1 week in 86% yield. Anal.

Calcd for $[LNi_2(\mu\text{-}OAcPh_2)]_2(ClO_4)_4 \cdot 3CH_3CN \cdot THF$ ($Ni_4C_{108}H_{109}N_{15}Cl_4O_{29}$): C, 52.78; H, 4.47; N, 8.55. Found: C, 52.67; H, 4.63; N, 8.68. Mp: 284−287 °C. UV−vis (CH_3CN, λ_{max}, nm (ε, $cm^{-1}\ M^{-1}$)): 363 sh (99), 588 (67), 993 (63). IR (KBr, cm^{-1}): 2072 (ν_{CN}), 1608 (ν_{py}), 1576 (ν_{py}), 1483, 1449, 1393, 1275, 1243, 1146 ($\nu_{ClO_4^-}$), 1117 ($\nu_{ClO_4^-}$), 1088 ($\nu_{ClO_4^-}$), 765, 707, 635 ($\nu_{ClO_4^-}$), 626 ($\nu_{ClO_4^-}$). ESI-MS (m/z, amu): 1032 $[L_2Ni_4(\mu\text{-}OAcPh)_2(ClO_4)_2]^{2+}$, 655 $[L_2Ni_4(\mu\text{-}OAcPh)_2(ClO_4)]^{3+}$, 466 $[L_2Ni_4(\mu\text{-}OAcPh)_2]^{4+}$.

General Procedure for the Conjugate Additions Catalyzed by Complex 1. To a blue acetonitrile solution (4 mL) of complex **1** (0.0164 g, 0.02 mmol) was added an α,β-enone (2.0 mmol) under a nitrogen atmosphere with stirring for 5 min. As the thiol (1.0 mmol) was added to the reaction mixture, the solution became brick red. The resulting solution was stirred at room temperature for 2 h, and the solvent was evaporated under vacuum. The residue was then purified by column chromatography on silica gel (hexane/AcOEt, 9/1) to give the conjugate adduct. Characterization of the conjugate addition products are listed in Supporting Information.

X-ray Structure Determination. Crystals of a suitable size for CCD X-ray diffractometry were selected under a microscope and mounted on the tip of a glass fiber fashioned on a copper pin. X-ray data for complexes **1** and **2** were collected on a Bruker-Nonius Kappa CCD diffractometer, and data for complexes **3** and **4** were collected on a Bruker Kappa Apex II diffractometer. Both instruments employed graphite-monochromated Mo Kα radiation (λ = 0.7107 Å) at 200 K and a $\theta-2\theta$ scan mode. The space groups for complexes **1**−**4** were determined on the basis of systematic absences and intensity statistics, and the structures of **1**−**4** were solved by direct methods using SIR92 or SIR97 and refined using SHELXL-97. Solvent molecules packing in the crystal lattices of **1**−**4** were severely disordered and were squeezed by the Platon program. An empirical absorption correction by multiscans was applied to all structures. All non-hydrogen atoms were refined with anisotropic displacement factors. Hydrogen atoms were placed in ideal positions and fixed with relative isotropic displacement parameters. Selected crystallographic data for **1**−**4** are given in Table 3, and their detailed crystallographic data are provided as CIF files in the Supporting Information. CCDC reference numbers are 737500, 750896, 737501, and 737502.

Magnetic Measurements. Variable-temperature dc magnetic susceptibility and ac magnetic susceptibility measurements were collected on microcrystalline samples, restrained in eicosane to prevent torquing, on a Quantum Design MPMS-XL SQUID magnetometer equipped with a 7.0 T magnet and operating in the range of 1.8−300.0 K. Diamagnetic corrections were estimated from Pascal's constants[20] and subtracted from the experimental susceptibility data to obtain the molar paramagnetic susceptibility of the compounds.

Acknowledgment. We acknowledge financial support from the National Science Council of Taiwan (Grant No. NSC 97-2113-M-003-004-MY2 to W.-Z.L.).

Supporting Information Available: CIF files giving X-ray crystallographic data for complexes **1**−**4** and text and figures giving additional details of the syntheses and ^1H and ^{13}C NMR data and spectra of the conjugate addition products. This material is available free of charge via the Internet at http://pubs.acs.org.

(20) Boudreaux, E. A.; Mulay, L. N. *Theory and Application of Molecular Paramagnetism*; Wiley: New York, 1976; p 491.